

Mice without uPA, tPA, or Plasminogen Genes Are Resistant to Experimental Choroidal Neovascularization

Jean-Marie Rakic,¹ Vincent Lambert,² Carine Munaut,² Khalid Bajou,² Karine Peyrollier,² Marie-Luz Alvarez-Gonzalez,² Peter Carmeliet,³ Jean-Michel Foidart,² and Agnès Noël²

¹Department of Ophthalmology, University Hospital, Sart-Tilman, Liège, Belgium;

²laboratory of Tumor and Development Biology, University of Liège, Liège, Belgium;

³Center for Transgene Technology and Gene Therapy, Flanders Interuniversity Institute for Biotechnology, University of Leuven, Belgium.

ABSTRACT

PURPOSE. To evaluate the presence and potential involvement of members of the plasminogen/plasminogen activator (Plg/PA) system in the exudative form of age-related macular degeneration (AMD).

METHODS. The expression of PA members mRNA was evaluated in human and experimental choroidal neovascularization (CNV) by RT-PCR. The presence and activity of PA was studied by immunofluorescence and in situ zymography. The influence of endogenous plasminogen (Plg), urokinase (uPA), tissue type plasminogen activator (tPA), and uPA receptor (uPAR) was explored in single-gene-deficient mice in a model of laser-induced CNV.

RESULTS. Members of the Plg/PA system were present both in human and murine CNV. The absence of Plg, uPA, or tPA significantly decreased the development of experimental CNV compared with wild-type or uPAR-deficient mice. This effect could be attributable, partly to a modulation of matrix metalloproteinase activity, but also to an accumulation of fibrinogen-fibrin in the laser-induced wounds.

CONCLUSIONS. Together with previous work done by the authors, this study indicates that choroidal neovascularization is extremely sensitive to the modulation of Plg/PA system activity. This may provide a new strategy for the treatment of exudative AMD.

Pathologic angiogenesis is the underlying cause of the exudative form of age-related macular degeneration (AMD). Unlike retinal neovascularization, choroidal neovascularization (CNV) is not primarily induced by hypoxia and the molecular signals involved in its initiation and progression are only partly defined.¹ Angiogenesis is an invasive process that requires proteolysis of the extracellular matrix, proliferation, and migration of endothelial cells with simultaneous synthesis of new matrix components. Such migratory and tissue remodeling events are regulated by different proteolytic systems including matrix metalloproteinases (MMPs) and serine proteinases of the plasminogen/plasminogen activator (Plg/PA) system.^{2,3} That MMPs are required for angiogenesis has been firmly established.⁴⁻⁶

Urokinase-type (uPA), which binds to a cellular receptor (uPAR), and tissue-type (tPA) plasminogen activators, are serine proteases both able to activate the zymogen plasminogen (Plg) into plasmin. Plasmin is a broadly acting enzyme that degrades fibrin and extracellular matrix proteins and activates pro-MMPs and growth factors.⁷ Plasminogen activator inhibitor type 1 (PAI-1) is the main physiological inhibitor of PA. Vascular endothelial growth factor (VEGF) induces uPA and tPA in endothelial cells derived from the microvasculature,⁸ and when endothelial cells migrate, they significantly upregulate uPA, tPA, uPAR, and PAI-1 at the leading edge of migration.^{2,9} The importance of PAI-1 in the "proteolytic balance" has been demonstrated in vitro¹⁰ and in tumoral angiogenesis.^{11,12} The specific roles of the Plg/PA system, however remain more controversial. Although developmental and wound-healing-associated angiogenesis was apparently unaffected in uPA-, uPAR-, tPA-, and Plg-deficient mice, several in vivo studies have demonstrated a requirement for this system in other settings.² This may indicate that the repertoire of active fibrinolytic proteins is likely to vary from one context to another.

The initial observation of a proangiogenic effect of uPA was reported in a model of corneal neovascularization.¹³ Several studies have later investigated the involvement of the fibrinolytic system in retinal neovascularization associated with diabetes.¹⁴⁻¹⁶ However, data concerning pathologic angiogenesis growing under the retina from the choroid are not available. We have previously reported the importance of PAI-1 expression in CNV.¹⁷ Because

neovascularization has been reported to occur on fibrin degradation in exudative AMD,^{18,19} we investigated here the expression and activity of members of the fibrinolytic system in human and laser-induced murine CNV. The influence of endogenous uPA, uPAR, tPA, and Plg on the formation of CNV was further evaluated in single-gene-deficient mice compared with wild-type (WT) control animals.

METHODS

RT-PCR Analysis of Neovascular Membranes

Eight consecutive submacular CNV specimens were completely removed during surgery for 360° macular translocation performed on patients with exudative AMD (three men, five women; mean age, 77 years; range, 72-83), either not amenable to conventional laser/photodynamic therapy (presence of occult new vessels or submacular bleeding) or in one patient, due to a severe recurrence a few months after a successful medical treatment (patients' demographics are given in Table 1). The neovascular membranes were snap frozen in liquid nitrogen and stored at 80°C. Intact human donor posterior segments (Cornea Bank, Liège, Belgium) were used as a control. The methods conformed to the Declaration of Helsinki for research involving human subjects.

TABLE 1. Patients Demographics

	M 71 (1)*	F 76 (2)	M 79 (3)	F 75 (4)
Preoperative visual acuity	20/200	20/400	20/1250	20/200
Subretinal hemorrhage	-	++	++	+
Lesize (DD)	1.5	2	4	3
CNV type (angiography)	Occult	ND	ND	Occult + PED
Previous therapy	-	-	PDT (2X)	-
Status of the other eye	Fibrotic CNV	Fibrotic CNV	Disciform scar	Dry AMD

DD, disc diameter; ND, not done; PED, pigment epithelium detachment; PDT, photodynamic therapy;

++ , refers to large amounts of blood preventing angiography.

* Gender and age are given with the number in brackets corresponding to the CNV membrane in Figure 1.

CNV was induced in mice by multiple argon laser burns, as previously described.²⁰ As a control, multiple subliminal laser burns (without the formation of the bubble sign) were also performed. Animals were killed at days 3, 5, 10, 14, 20, and 40, and the eyes were enucleated. The posterior segments (neural retina and RPE-choroid complex) were dissected and immediately frozen in liquid nitrogen.

The frozen tissues were pulverized in a dismembrator (B. Braun Biotech International, GmbH, Melsungen, Germany), and total RNA was isolated with an extraction kit (RNeasy; Qiagen, Paris, France) according to the manufacturer's protocol. 28S rRNA was amplified with an aliquot of 10 ng total RNA with an RNA PCR kit (GeneAmp ThermoStable rTth reverse transcriptase; Applied Biosystems, Foster City, CA) and two pairs of primers (Eurogentec, Liège, Belgium; oligonucleotides sequences are shown in Table 2). Reverse transcription was performed at 70°C for 15 minutes, followed by a 2-minute incubation at 95°C for denaturation of RNA-DNA heteroduplexes. Amplification started at 15 seconds at 94°C, 20 seconds at 60°C, and 10 seconds at 72°C. RT-PCR products were resolved on 2% agarose gels and analyzed with a fluorescence imager (Fluor-S Multimag; Bio-Rad, Richmond, CA) after staining with ethidium bromide (FMC BioProd-ucts, Philadelphia, PA).

Murine Model of Laser-Induced CNV

CNV was induced in mice by four burns (at the 6, 9, 12, and 3 o'clock positions around the optic disc) using a green argon laser (532 nm; 50-μm diameter spot size; 0.05-second duration; 400-mW intensity).¹⁷ Eyes in which no bubble developed at the site of laser treatment or in which there was subretinal bleeding were not included in the analysis. The eyes were enucleated at day 14, embedded in mounting medium (Tissue Tek; Miles Laboratories, Naperville, IL), and frozen in liquid nitrogen for cryostat sectioning. CNV was quantified as previously described.^{17,20} Briefly, frozen serial sections were cut throughout the entire extent of each burn, and the thickest region (minimum of four per lesion) was used for the quantification. Using a computer-assisted image analysis system (Olympus Micro Image version 3.0 for Windows 95/NT, Olympus Optical Co., London, UK), neovascularization was estimated by the ratio B/C: thickness from the bottom of the pigmented choroidal layer to the top of the neovascular membrane (B)/ thickness of the intact pigmented choroid adjacent to the lesion (C).

Genetically Modified Mice

Brother-sister mating generated all knockout mice in a C57BL/6/129 background and their corresponding WT littermates. Homozygous mice deficient of uPA (uPA^{-/-}), tPA (tPA^{-/-}), uPAR (uPAR^{-/-}), and Plg (Plg^{-/-}) and their corresponding WT littermates with a mixed genetic background of 75% C57BL6 and 25% 129 SV/SL strain were generated as described previously.²¹⁻²³ Mice of either sex aged between 8 and 12 weeks were used. There were five or more mice in each group. The animals were maintained in a 12-hour light-dark cycle and had free access to food and water. All the animal experiments were performed in compliance with the Association for Research in Vision and Ophthalmology (ARVO) statement for the Use of Animals in Ophthalmic and Vision Research.

Immunohistochemistry

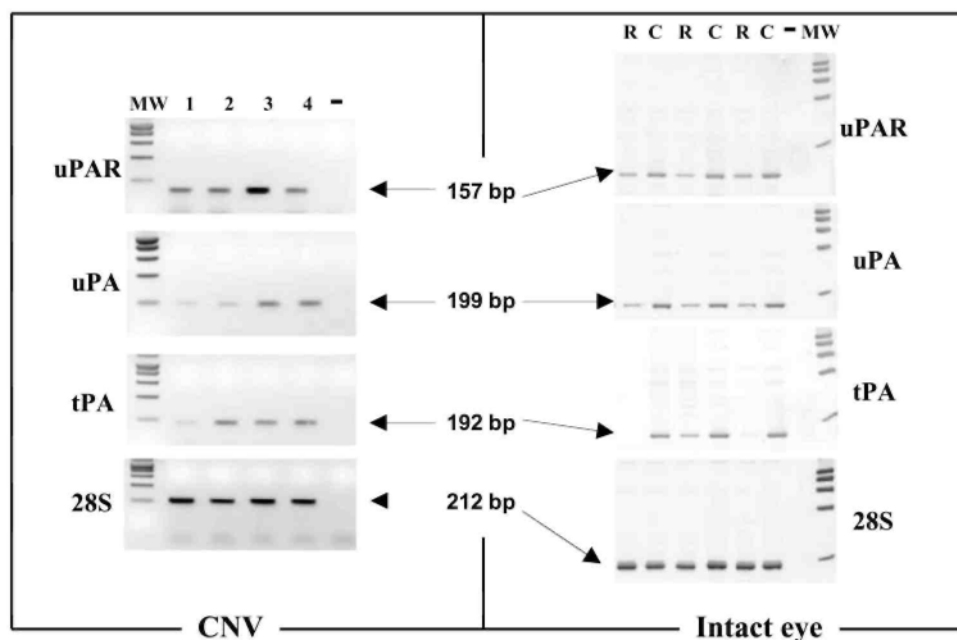
Cryostat sections (5- μ m thick) were fixed in paraformaldehyde 1% in 0.07 M phosphate-buffered saline (PBS; pH 7.0) for 5 minutes or in acetone for 10 minutes at room temperature and then incubated with the primary antibody. Antibodies raised against type IV collagen (guinea pig polyclonal, produced in our laboratory; diluted 1:100), mouse platelet- endothelial cell adhesion molecule (PECAM; rat mono-clonal, PharMingen, San Diego, CA; diluted 1:20), murine uPA (rabbit polyclonal, a generous gift of Peter Carmeliet, Catholic University, Leuven, Belgium; diluted 1:500), murine tPA (rabbit polyclonal, a generous gift of Peter Carmeliet; diluted 1:500), murine uPAR (rabbit polyclonal, a generous gift of Steve Rosenberg, Chiron Corp., Emeryville, CA.; diluted 1:500) and murine fibrinogen-fibrin (goat polyclonal; Nordic Immunologic, Tilburg, The Netherlands; diluted 1:400) were incubated for 1 hour at room temperature. The sections were washed in PBS (3 \times 10 minutes) and the appropriate secondary antibody was added, conjugated to horse radish peroxidase (HRP), tetramethyl-rhodamine isothiocyanate (TRITC), or fluorescein-isothio-cyanate (FITC): rabbit anti-goat IgG (Dako, Glostrup, Denmark, diluted 1:100), rabbit anti-rat IgG (Sigma-Aldrich, Bornem, Belgium; diluted 1:40), swine anti-rabbit IgG (Dako; diluted 1:200), monoclonal anti-guinea pig IgG (Sigma-Aldrich, Belgium; diluted 1:200) were applied for 30 minutes. For staining of fibrinogen-fibrin, a drop of 3-amino-9-ethylcarbazole (AEC⁺; Dako) was added, and sections were counter-stained for 1 minute with hematoxylin. For immunofluorescence staining, after three washes in PBS for 10 minutes each and a final rinse in 10 mM Tris-HCl buffer (pH 8.8), labeling was analyzed under an inverted microscope equipped with epifluorescence optics. Specificity of staining was assessed either by substitution of nonimmune serum for primary antibody or by testing in the deficient animal.

TABLE 2. RT-PCR Parameters

Gene (Accession No.)	Position	Oligonucleotide Sequence (C5'-3')	Size of PCR Product (bp)	Cycles (n)
28S (U13369)	12403F 12614R	GTTCACCCACTAATAGGGAACGTGA GGATTCTGACTTAGAGGCGTTCAGT	212b	19
h uPA (X02419)	5020F 6209R	ACTACTACGGCTCTGAAGTCACCA GAAGTGTGAGACTCTCGTGTAGAC	199b	33
m uPA (M17922)	6527F 8016R	TATGCAGCCCCACTACTATGGCTC GAAGTGTGAGACTCTCGTGTAGAC	210b	35
h tPA(M15518)	146F 337R	CAGGAAATCCATGCCCGATT GCTGCAACTTTTGACAGGCAC	192b	33
m tPA 003520)	192F 391R	CTACAGAGCGACCTGCAGAGAT AATACAGGGCCTGCTGACACGT	200b	35
h uPAR (U08839)	901F 1057R	CTGGAGCTTGAAAATCTGCCG GGTTTTTCGGTTCGTGAGTGC	157b	33
m uPAR (X62700)	156F 289R	ACTACCGTGCTTCGGGAATG ACGGTCTCTGTCAGGCTGATG	134b	35

m and h, mouse and human, respectively.

FIGURE 1. PA expression in exudative AMD. Representative example of uPAR, uPA, and tPA mRNA expression in surgically extracted choroidal neovascular membranes of patients 1 to 4 (left, lanes 1-4, respectively), who had exudative AMD (Table 1) or in posterior segments of intact donors. Total RNA (approximately 10 ng) was analyzed by RT-PCR. The 28S rRNA was used to assess the total amount of RNA loaded. Lane M: molecular markers. Product size (bp) are shown at right. Right: lane R: neural retina; lane C: choroid-RPE complex.



In Situ Casein Zymography

Cryostat sections were coated with a mixture containing 2% skim milk, 0.9% agar, and 600 μ L Pig (Sigma-Aldrich), as previously described.^{11,12} An 8% milk stock solution was prepared in PBS, heated at 95 °C for 30 minutes, and centrifuged at 3000 rpm to remove insoluble material. Slides were incubated at 37°C in a humidified chamber for 4 hours for assessment of total PA activity and for 24 hours in the presence of uPA-specific inhibitor amiloride (2 mM; Sigma-Aldrich) for assessment of tPA activity. Caseinolysis was monitored by examination under a dark-field microscope.

Gelatin Zymography Assay

CNV was induced in mice by multiple laser burns, as described earlier. Animals were killed at day 3, and the eyes were enucleated. The posterior segments were dissected and snap frozen in liquid nitrogen. Frozen tissues were then pulverized in liquid nitrogen, homogenized in buffer (0.1 M Tris-HCl [pH8.1] and 0.4% Triton X-100) and centrifuged for 20 minutes at 5000g. The pellets were discarded. Aliquots of supernatants were mixed with SDS sample buffer and electrophoresed directly as previously described.²⁴ All lanes were loaded with equal amounts of material (5 ng).

Statistical Analysis

Data were analyzed on computer (Prism 30; GraphPad, San Diego, CA). The Mann-Whitney test was used to determine whether there were significant ($P < 0.05$) differences between control and genetically modified mice.

RESULTS

RT-PCR Analysis of Neovascular Membranes

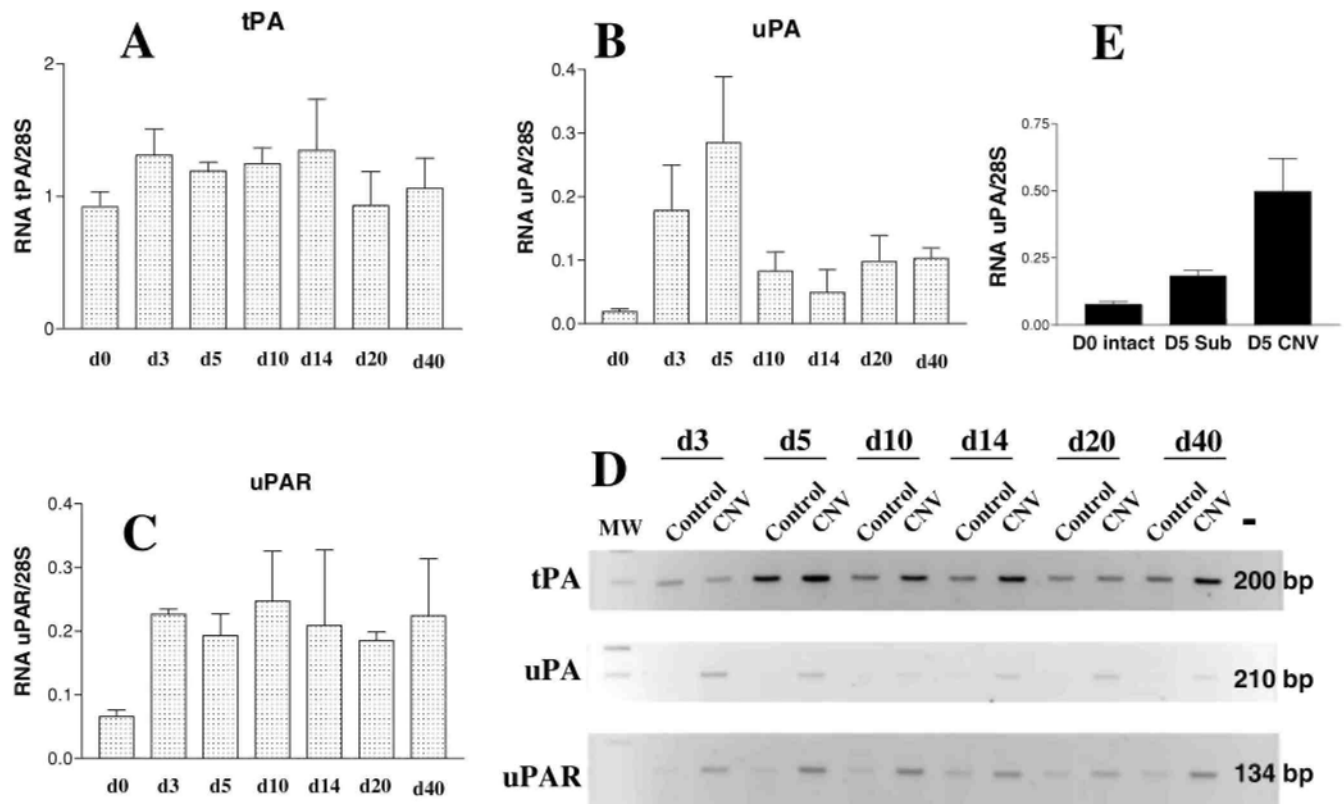
uPA, tPA, and uPAR mRNAs were detected in all CNV specimens obtained during surgery. However, basal expression of these mRNAs was also documented in intact donors, as previously described^{26,27} (Fig. 1). Patients with these aggressive neovascular membranes had a documented (Table 1) different natural history (size of the

lesion, amount of blood, previous treatment). Expression of PA mRNA seemed to be relatively increased in patients with larger lesions or with significant amounts of blood in the subretinal space. To evaluate more precisely the temporal pattern of gene expression, semiquantitative RT-PCR analysis (normalized to 28S signal) was then applied on laser-induced murine neovascular choroidal membranes at different end points (days 3-40 after laser treatment). As shown on densitometry histograms (Figs. 2A-C), uPA and uPAR mRNAs displayed the largest induction during the course of experimental murine CNV, with a decrease in expression after day 10 (coinciding with the period of CNV stabilization). A similar induction was not observed when low-power laser treatment (not disrupting Bruch's membrane) was applied (Fig. 2E).

Presence of uPA, tPA, and uPAR in Experimental CNV

Immunohistochemical staining demonstrated the presence of uPA, tPA, and uPAR proteins at the site of laser-induced injury (RPE and choroidal layer, Figs. 3A-C). No staining was observed at any location in uPA^{-/-}, tPA^{-/-}, or uPAR^{-/-} mice (not shown). uPAR protein was detected both in CNV and in adjacent intact areas (Fig. 3B). In situ zymography in WT mice revealed that PA activity was mainly localized in and around the laser-induced CNV (Fig. 3E), but was also present (after a longer incubation) at the RPE layer (Fig. 3F). Caseolytic activity was also detected (at a weaker level) when uPA was inhibited with amiloride, suggesting that tPA mediates a part of the observed proteolytic effect (Fig. 3G).

FIGURE 2. RT-PCR analysis of PA mRNA expression during the development of murine laser-induced CNV. The histograms correspond to the densitometric quantification of tPA (A), uPA (B), and uPAR (C) mRNA normalized to the 28S signal at different end points. The evaluation was performed on the entire posterior segment after the induction of multiple wounds to Bruch's membrane. As a control, a similar evaluation was performed for uPA at day 5 with multiple subliminal laser impacts (E). D5sub, subliminal laser treatment; D5 CNV, laser treatment with rupture of the Bruch's membrane. Unlike tPA which remained relatively constant, expression of uPA and uPAR mRNA appeared to be induced during the early phases of development of CNV. Representative gels are displayed with molecular size markers (bp) at right (D).



CNV Development In Vivo in uPA^{-/-}, tPA^{-/-}, uPAR^{-/-} and Plg^{-/-} Mice

To determine whether the absence of members of the PA^{-/-}Plg system influences CNV in vivo, we evaluated the severity of the neovascular reactions by immunostaining with anti-PECAM antibodies and, histologically, by measuring, on serial sections, the maximum height of the lesion above the choroidal layer observed in neighboring intact zones.^{17,20} CNV at the site of laser-induced trauma was very restricted in uPA^{-/-}, tPA^{-/-} (not shown), and Plg^{-/-} mice, but robust CNV was observed in uPAR^{-/-} and WT (not shown) mice (Figs. 4A-C). This was quantified by determining the B/C ratio between total thickness of lesions to the thickness of adjacent normal choroid, and an approximately 50% reduction of the B/C ratio was consistently observed in uPA^{-/-}, tPA^{-/-}, and Plg^{-/-} mice ($P < 0.001$) compared with WT mice (Fig. 4D).

Gelatin Zymography Assay

To investigate an influence on matrix metalloproteinase (MMP) activity due to the absence of PA or Plg, the activities of MMP-2 and -9 in control and deficient mice were analyzed by gelatin zymography performed on the posterior segment after multiple laser-induced trauma. The latent form of MMP-2 (known to be constitutively expressed) was detected in all tissue extracts (Fig. 5). MMP-9 activity was not detected in intact eyes, whereas higher levels were found in laser-treated eyes. However, MMP-9 activity appeared to be decreased and that of MMP-2 increased in Plg/PA^{-/-} mice compared with WT control animals.

Fibrinogen/Fibrin Deposition in uPA^{-/-}, tPA^{-/-}, and Plg^{-/-} Mice

Mice with a single deficiency of tPA or uPA are susceptible to thrombosis after traumatic or inflammatory challenge,²¹ and it has been demonstrated that fibrinogen is responsible for the phenotype observed in Plg^{-/-} mice.²⁵ Therefore, to explore the possibility that excessive fibrinogen-fibrin deposition could be responsible for the decreased choroidal angiogenesis observed in Plg/PA^{-/-} mice, fibrinogen-fibrin was immuno-stained at day 3 after laser treatment (Figs. 6A-D). Although WT control animals showed a modest fibrinogen-fibrin presence on the CNV's forward edge, uPA^{-/-}, tPA^{-/-}, and Plg^{-/-} mice demonstrated massive accumulation of fibrinogen-fibrin both in the retinal vessels, and in the bottom of the laser-induced trauma, which had a "sealed" appearance.

DISCUSSION

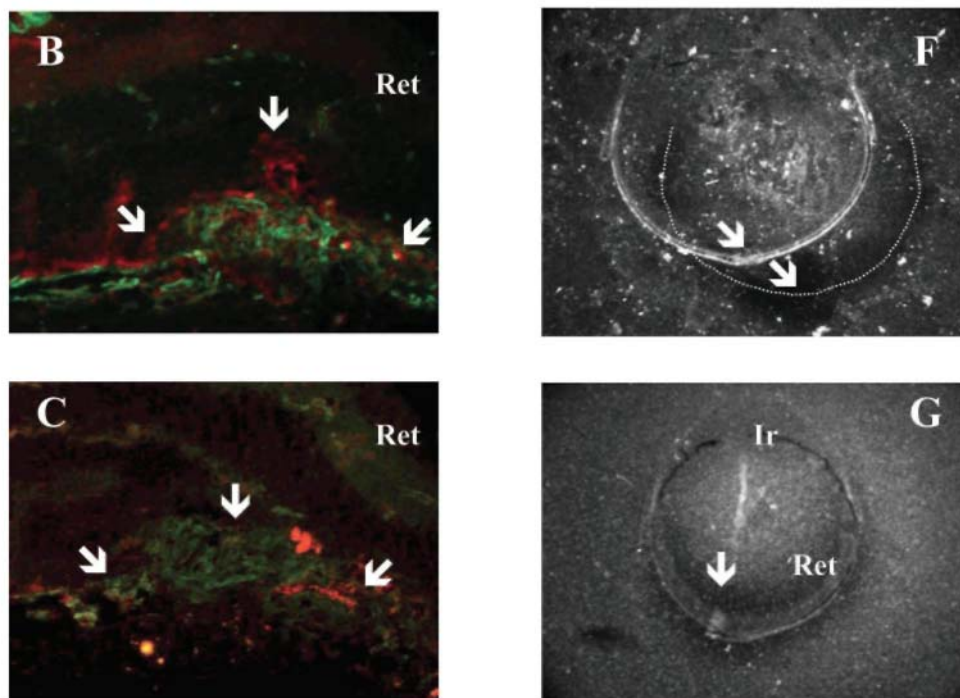
Our data report for the first time the expression of tPA, uPA, and uPAR mRNAs, both in choroidal neovascular membranes surgically extracted from patients with exudative AMD and during murine experimental CNV. This suggests (but does not definitively show) that these molecules may be involved in the CNV process in humans, because basal expression of these molecules was also present (primarily in the choroid-RPE complex) in intact eyes (Fig. 1). These observations were extended in mice by immunostaining and in situ zymography showing PA activity at the site of laser-induced trauma. We investigated therefore the influence of a deficiency in the Plg/PA system on the development of experimental CNV.

WT control mice and uPAR^{-/-} mice exhibited a robust angiogenic response. However, significant experimental CNV did not develop in uPA^{-/-}, tPA^{-/-}, or Plg^{-/-} animals, suggesting a contribution of these proteinases in chorioretinal disease. Indeed, it has been demonstrated that the intact choroid is a source of continuous tPA secretion²⁶ and the RPE a source of uPA.²⁷ Urokinase activity was increased in experimental retinal neovascularization and in diabetic neovascular membranes.^{15,28} Intraocular elevated tPA levels have been associated with proliferative diabetic retinopathy,¹⁶ and preliminary observations have suggested that uPA inhibition could prevent the retinal neovascularization induced by hypoxia (Mcguire PG, Jones TR, Talaric N, Warren E, Das A, ARVO Abstract 1261, 2002). The apparent absence of effect secondary to uPAR deficiency may be explained by the observation that binding of uPA to uPAR is not required to provide sufficient pericellular uPA-mediated plasmin proteolysis.²⁹

The phenotype observed in uPA^{-/-}, tPA^{-/-}, and Plg^{-/-} mice could not be directly ascribed to a defect at the endothelial level. Indeed, first, CNV is not a disease exclusively caused by isolated endothelial cell pathologic proliferation. Clinical and experimental data^{20,30} have shown the presence of an important inflammatory component in the disease, suggesting that CNV is a nonspecific wound-healing response.³¹ Second, previous studies have showed that endothelial cell migration in fibrin gels is not severely impaired by isolated deficiency of Plg/PA system components, but is an essential active membrane-type 1 MMP.³² That deficiencies in endogenous uPA or tPA does not impair endothelial cell migration has been confirmed in the aortic ring model¹⁰ and in a

model of tumoral angiogenesis induced by implantation of malignant keratinocytes.¹² Nevertheless, angiogenesis in these two models was still dependent on the presence of Plg, indicating that plasmin-mediated proteolysis may be a key event in particular experimental settings. In addition, while defective pathologic angiogenesis in uPA^{-/-} and tPA^{-/-} mice has not been reported for a while, recent data challenge this observation.

FIGURE 3 Presence and activity of PA in murine CNV. Immunolocalization (red) of uPA (A), uPAR (B), and tPA (C) in ocular frozen sections counterstained with collagen type IV antibody (green) at day 14 after laser injury of Bruch's membrane in WT mice. In situ zymography of ocular sections in WT mice at day 3 after laser treatment. Total PA activity was visualized as a dark zone of lysis (dark-field images) after incubation for 4 (E) and 12 (F) hours. After 12 hours, the localization of PA extended in the intact RPE (the retracted casein gel has moved to the right side of the slide). In the presence of 2 mM amiloride for 24 hours, only tPA activity was detected (G). Negative control (D). Ret, neural retina; Le, lens; and Ir, iris; arrows: neo-vascular area. Original magnification: (A-C) X400; (E-G) X25.



Recently, a critical role for tPA during invasion and angiogenesis of pancreatic tumor cells has been suggested.³³ Furthermore, the presence of uPA or Plg is essential for capillary angiogenesis during infarct revascularization.³⁴ This particular phenotype is partly explained by defective MMP-9 activation in the infarcted heart secondary to the absence of uPA and plasmin. In our model, MMP-9 appeared to be decreased, whereas MMP-2 activity seemed to be increased when Plg/PA was deficient (Fig. 5). All together, these data support the idea that the need for PA during angiogenesis may be related to the composition of the extracellular matrix or to the expression pattern of proteinases during different conditions.

PAI-1 is the main physiological inhibitor of uPA and tPA. It not only regulates the proteolytic activity of uPA but also determines the level of uPA bound to its cell surface receptor (uPAR) by promoting the rapid endocytosis of the trimolecular uPA-uPAR-PAI-1 complex.³⁵ We have reported previously that deficient expression of PAI-1 in mice prevents the development of experimental CNV, which is restored when systemic and local PAI-1 expression is achieved by intravenous injection of a replication-defective adenoviral vector expressing PAI-1 cDNA.¹⁷ However, high doses of PAI-1 were equally efficient in inhibiting development of CNV (Lambert V, Munaut C, Bajou K, et al., manuscript submitted) indicating that in this murine model of exudative AMD, finely tuned fibrinolysis was a key element. In the current study, immunohistochemically that in the absence of uPA, tPA, or Plg, excessive accumulation of fibrinogen-fibrin took place at the level of the laser-induced trauma, even in the presence of MMP activity. These fibrin deposits may impose a physical barrier to several components of normal CNV (endothelial cells, fibroblasts, and monocytes) that cannot be resolved without plasmin-mediated fibrinolysis. Taken together, these results suggest that in the choroid, the angiogenic program is more dependent on the PA/Plg axis than on MMP-driven fibrinolysis. This is in line with our recent observations in MMP-9 - deficient mice

showing that, although MMP-9 is expressed and active during development of CNV, its absence induces only a modest reduction in neovascularization.²⁰

Choroidal capillaries forming pathologic neovascular membranes appear to be exquisitely sensitive to variations in the proteolytic PA-driven balance. Both excessive fibrinolysis (such as occurred in PAI-1 deficiency) and defective fibrinolysis (the result of either isolated Plg/PA deficiency, or excessive PAI-1 levels) prevents the development of neovascularization and could be proposed, if appropriately controlled, as an antiangiogenic pharmacologic strategy.

FIGURE 4. Absence of Plg, uPA, or tPA prevents the development of CNV. Hematoxylin-eosin staining of a representative area of CNV at the site of laser-induced trauma in mice deficient of uPAR (A), uPA (B), and Plg (C). Neovascularization was almost completely absent in uPA^{-/-} (F) and Plg^{-/-} (G) mice when vessels were immunostained with anti-mouse PECAM antibody (green) compared with WT (not shown) or uPAR^{-/-} (E) mice. Ret, neural retina; Ch, choroid; arrows: neovascular area. (D) The neovascular reaction was determined with computer-assisted image analysis by evaluating the B/C ratio, as described previously,^{17,20} at day 14 after laser injury of Bruch's membrane in WT and gene-deficient mice. ***P < 0.001; error bars = SE. Original magnification: (A-C) X200; (E, F, G) X400.

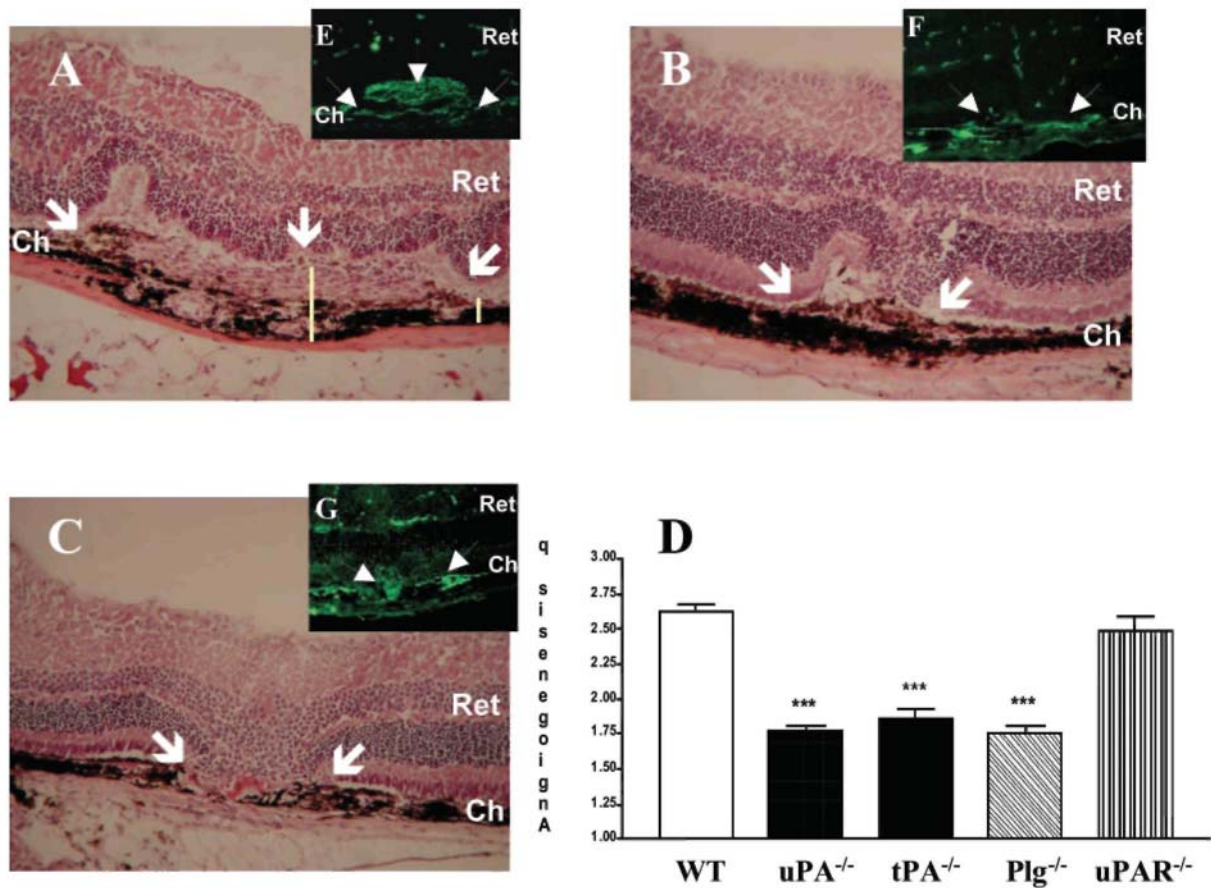


FIGURE 5. Zymographic analysis of MMP-2 and -9 in Plg/PA^{-/-} and WT mice. Tissues were extracted either from posterior eyes segments with laser-induced neovascularization or intact eyes of three different mice. As a positive control, medium conditioned by human HT1080 cells was included. All lanes were loaded with the same amount of material (5 ng).

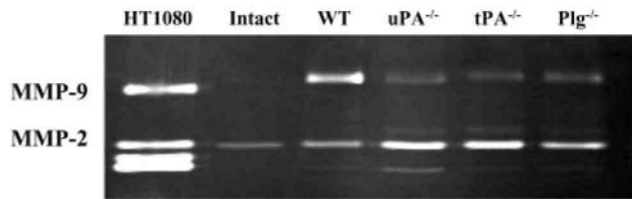
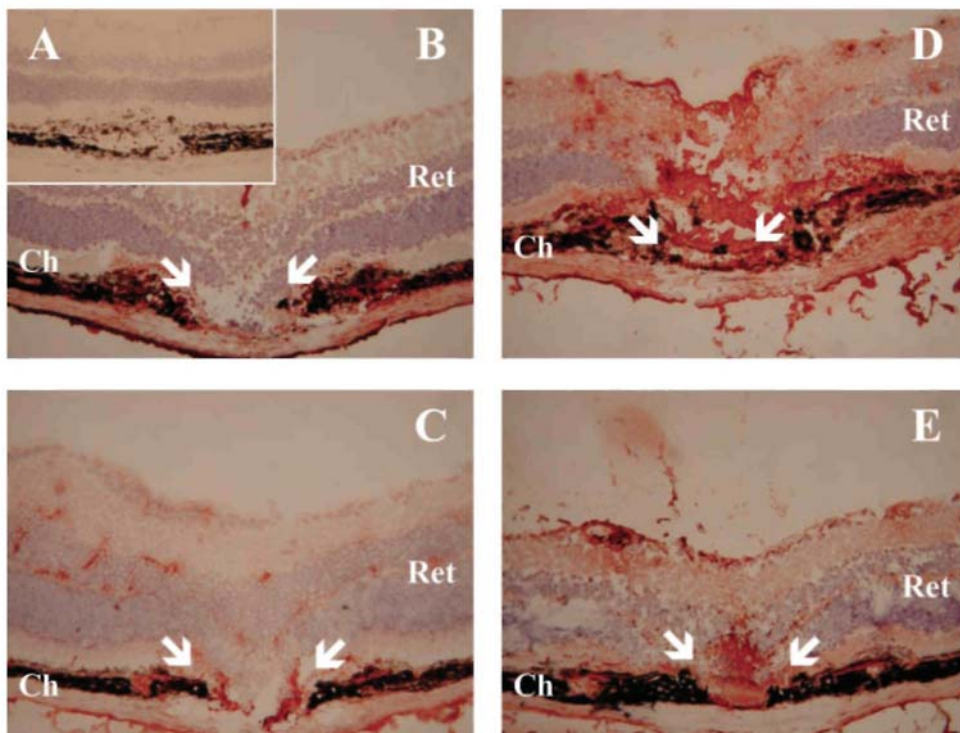


FIGURE 6. Immunohistochemical staining for fibrinogen-fibrin at the site of a laser-induced wound. Frozen ocular sections from wild-type (B), uPA^{-/-} (C), tPA^{-/-} (D), and Plg^{-/-} (E) mice reveal the presence of limited amount of fibrin in WT mice, contrasting with the accumulation of fibrin in Plg/PA-system-deficient mice both at the site of choroidal trauma and in retinal vessels. Negative control (A). Original magnification, X200.



ACKNOWLEDGMENTS

The authors thank Laurent Naa and Fabrice Olivier for collaboration in the study and Patricia Gavitelli for technical assistance.

Supported by grants from the European Commission (FP4 and FP5 Programs), the Fund for Medical Scientific Research, the National Fund for Scientific Research (FNRS, Belgium), the Belgian Federation against Cancer, the FB Assurances, the Léon Frédéricq Foundation (University of Liège), the Fund for Investment in Scientific Research (Liège, Belgium), and the Interuniversity Attraction Poles (IUAP) from the Federal Office for Scientific, Technical, and Cultural Affairs, Brussels, Belgium.

Disclosure: J.-M. Rakic, None; V. Lambert, None; C. Munaut, None; K. Bajou, None; K. Peyrollier, None; M.-L. Alvarez-Gonzalez, None; P. Carmeliet, None; J.-M. Foidart, None; A. Noël, None

The publication costs of this article were defrayed in part by page charge payment. This article must therefore be marked "advertisement" in accordance with 18 U.S.C. §1734 solely to indicate this fact.

REFERENCES

1. Campochiaro PA. Retinal and choroidal neovascularization. *J Cell Physiol.* 2000;184:301-310.
2. Pepper MS. Role of the matrix metalloproteinase and plasminogen activator-plasmin systems in angiogenesis. *Arterioscler Thromb Vasc Biol.* 2001;21:1104-1117.
3. Blasi F. Proteolysis, cell adhesion, chemotaxis, and invasiveness are regulated by the u-PA-u-PAR-PAI-1 system. *Thromb Haemost.* 1999;82:298-304.
4. Stetler-Stevenson WG. Matrix metalloproteinases in angiogenesis: a moving target for therapeutic intervention. *J Clin Invest.* 1999;103:1237-1241.
5. Bergers G, Brekken R, McMahon G, et al. Matrix metalloproteinase-9 triggers the angiogenic switch during carcinogenesis. *Nat Cell Biol.* 2000;2:737-744.
6. Egeblad M, Werb Z. New functions for the matrix metalloproteinases in cancer progression. *Nat Rev Cancer.* 2002;3:161-174.
7. Andreasen PA, Kjoller L, Christensen L, Duffy MJ. The urokinase-type plasminogen activator system in cancer metastasis: a review. *Int J Cancer.* 1997;72:1-22.
8. Cavallaro U, Tenan M, Castelli V, et al. Response of bovine endothelial cells to FGF-2 and VEGF is dependent on their site of origin: relevance to the regulation of angiogenesis. *J Cell Biochem.* 2001; 82:619-633.
9. Carmeliet P, Collen D. Genetic analysis of blood vessel formation: role of endothelial versus smooth muscle cells. *Trend Cardiovasc Med.* 1997;7:271-281.
10. Devy L, Blacher S, Grignet-Debrus C, et al. The pro- or antiangiogenic effect of plasminogen activator inhibitor 1 is dose dependent. *FASEBJ.* 2002;16:147-154.
11. Bajou K, Noel A, Gerard RD, et al. Absence of host plasminogen activator inhibitor 1 prevents cancer invasion and vascularization. *Nat Med.* 1998;4:923-928.
12. Bajou K, Masson V, Gerard RD, et al. The plasminogen activator inhibitor PAI-1 controls in vivo tumor vascularization by interaction with proteases, not vitronectin: implications for antiangiogenic strategies. *J Cell Biol.* 2001;152:777-784.
13. Berman M, Winthrop S, Ausprunk D, Rose J, Langer R, Gage J. Plasminogen activator (urokinase) causes vascularization of the cornea. *Invest Ophthalmol Vis Sci.* 1982;22:191-199.
14. Grant MB, Guay C. Plasminogen activator production by human retinal endothelial cells of nondiabetic and diabetic origin. *Invest Ophthalmol Vis Sci.* 1991;32:53-64.
15. Das A, McGuire PG, Eriqat C, et al. Human diabetic neovascular membranes contain high levels of urokinase and metalloproteinase enzymes. *Invest Ophthalmol Vis Sci.* 1999;40:809-813.
16. Hattenbach LO, Allers A, Gumbel HO, Scharrer I, Koch FH. Vitreous concentrations of TPA and plasminogen activator inhibitor are associated with VEGF in proliferative diabetic vitreoretinopathy. *Retina.* 1999;19:383-389.
17. Lambert V, Munaut C, Noel A, et al. Influence of plasminogen activator inhibitor type I on choroidal neovascularization. *FASEBJ.* 2001;15:1021-1027.
18. Lopez PF, Grossniklaus HE, Lambert HM, et al. Pathologic features of surgically excised subretinal neovascular membranes in age-related macular degeneration. *Am J Ophthalmol.* 1991;112:647-656.
19. Lopez PF, Lambert HM, Grossniklaus HE, Sternberg P Jr. Well-defined subfoveal choroidal neovascular membranes in age-related macular degeneration. *Ophthalmology.* 1993;100:415-422.
20. Lambert V, Munaut C, Noël A, Werb Z, Foidart J-M, Rakic J-M. MMP-9 contributes to choroidal neovascularization. *Am J Pathol.* 2002;161:1247-1253.
21. Carmeliet P, Schoonjans L, Kieckens L, et al. Physiological consequences of loss of plasminogen activator gene function in mice. *Nature.* 1994;368:419-424.
22. Carmeliet P, Collen D. Development and disease in proteinase-deficient mice: role of the plasminogen, matrix metalloproteinase and coagulation system. *Thromb Res.* 1998;91:255-285.

23. Ploplis VA, French EL, Carmeliet P, Collen D, Plow EF. Plasminogen deficiency differentially affects recruitment of inflammatory cell populations in mice. *Blood*. 1998;91:2005-2009.
24. Munaut C, Noel A, Weidle UH, Krell HW, Foidart JM. Modulation of the expression of interstitial and type-IV collagenases in coculture of HT1080 fibrosarcoma cells and fibroblasts. *Invasive Metastasis*. 1995;15:169-178.
25. Bugge TH, Kombrinck KW, Flick MJ, Daugherty CC, Danton MJ, Degen JL. Loss of fibrinogen rescues mice from the pleiotropic effects of plasminogen deficiency. *Cell*. 1996;87:709-719.
26. Wang Y, Gillies C, Cone RE, O'Rourke J. Extravascular secretion of t-PA by the intact superfused choroid. *Invest Ophthalmol Vis Sci*. 1995;36:1625-1632.
27. Hackett SF, Campochiaro PA. Modulation of plasminogen activator inhibitor-1 and urokinase in retinal pigmented epithelial cells. *Invest Ophthalmol Vis Sci*. 1993;34:2055-2061.
28. Das A, McLamore A, Song W, McGuire PG. Retinal neovascularization is suppressed with a matrix metalloproteinase inhibitor. *Arch Ophthalmol*. 1999;117:498-503.
29. Carmeliet P, Moons L, Dewerchin M, et al. Receptor-independent role of urokinase-type plasminogen activator in pericellular plasmin and matrix metalloproteinase proteolysis during vascular wound healing in mice. *J Cell Biol*. 1998;140:233-245.
30. Grossniklaus HE, Cingle KA, Yoon YD, Ketkar N, L'Hernault N, Brown S. Correlation of histologic 2-dimensional reconstruction and confocal scanning laser microscopic imaging of choroidal neovascularization in eyes with age-related maculopathy. *Arch Ophthalmol*. 2000;118:625-629.
31. Spraul CW, Lang GE, Grossniklaus HE, Lang GK. Histologic and morphometric analysis of the choroid, Bruch's membrane, and retinal pigment epithelium in postmortem eyes with age-related macular degeneration and histologic examination of surgically excised choroidal neovascular membranes. *Surv Ophthalmol*. 1999;44:10-32.
32. Hiraoka N, Allen E, Apel IJ, Gyetko MR, Weiss SJ. Matrix metallo-proteinases regulate neovascularization by acting as pericellular fibrinolysins. *Cell*. 1998;95:365-377.
33. Diaz VM, Planaguma J, Thomson TM, Reventos J, Paciucci R. Tissue plasminogen activator is required for the growth, invasion, and angiogenesis of pancreatic tumor cells. *Gastroenterology*. 2002;122:806-819.
34. Heymans S, Luttun A, Nuyens D, et al. Inhibition of plasminogen activators or matrix metalloproteinases prevents cardiac rupture but impairs therapeutic angiogenesis and causes cardiac failure. *Nat Med*. 1999;5:1135-1142.
35. Rifkin DB, Mazzieri R, Munger JS, Noguera I, Sung J. Proteolytic control of growth factor availability. *APMIS*. 1999;107:80-85.